

Contact Transfer: A Direct, User-Driven Method for Human to Robot Transfer of Grasps and Manipulations

Arjun Lakshminpathy¹ Dominik Bauer² Cornelia Bauer² Nancy S. Pollard^{1,2}

Abstract—We present a novel method for the direct transfer of grasps and manipulations between objects and hands through utilization of contact areas. Our method fully preserves contact shapes, and in contrast to existing techniques, is not dependent on grasp families, requires no model training or grasp sampling, makes no assumptions about manipulator morphology or kinematics, and allows user control over both transfer parameters and solution optimization. Despite these accommodations, we show that our method is capable of synthesizing kinematically feasible whole hand poses in seconds even for poor initializations or hard to reach contacts. We additionally highlight the method’s benefits in both response to design alterations as well as fast approximation over in-hand manipulation sequences. Finally, we demonstrate a solution generated by our method on a physical, custom designed prosthetic hand.

I. INTRODUCTION

Transfer of human grasps and manipulation demonstrations to robot hands has been a long standing and challenging problem in the robotics community. Though numerous anthropomorphic hands have been developed (e.g., [9], [7], [19], [6], [8], [12]), no current manipulator yet matches the dexterous capabilities of the human hand. In addition, simpler hands are often desired based on considerations such as weight, cost, and ease of manufacture and control.

Towards this end, many research efforts have endeavored to develop methods for robustly transferring dexterous capabilities to robot hands with characteristics that may differ from the hand of the human demonstrator. The majority of existing methods fall into pure learning, hand pose tracking and retargeting, or a hybrid of both. Pure reinforcement learning methods have produced convincing results even for complex manipulations [36], [46], [10], but occasionally yield policies with unexpected or undesirable behaviors due to the abstract nature of the reward function. Tracking methods instead capture the movements of both the human hand and the object being manipulated with the intention of grounding the learned policy [25] or directly transferring the motion to the target manipulator [11], [20]; unfortunately, occlusion and noise during the tracking process, as well as morphological differences between the human and target hand, complicate the process.

Contacts instead present an alternate and often complementary means of encoding grasps and manipulations. Historical works have used contact information to prune kinematically infeasible solutions [34], match object and hand shapes [31], [24], and drive physics based reasoning

[44]. Recent works exploit entire contact regions to synthesize grasps for morphologically diverse manipulators [15], optimize coarse poses [21], and help train pose generation models [26]. The catch, however, is that most existing techniques incur one of three possible drawbacks: single point approximation [34], [31], [24], [44], strong dependence on grasp dependent hand shape priors [21], [26], or expensive computation due to exhaustive grasp sampling [15].

In response to these drawbacks, we present a method that is not dependent on hand shape priors or grasp sampling, instead exploiting the key idea, backed by ground truth observations [16], that contact areas can often be strongly associated with a particular hand region (i.e. palm, individual finger, etc.), even if the target manipulator is not anthropomorphic. This paper thus makes the following contributions:

- 1) a novel approach to *directly* transfer contact areas of arbitrary shape to morphologically diverse manipulators in a fast and fully customizable manner
- 2) a cheap optimization strategy to quickly synthesize kinematically feasible grasps and in-hand manipulations by exploiting correspondences generated by the transfer process

Additionally, we demonstrate that our method can accommodate hands with high degrees of freedom and contact areas of widely varying shapes. We also show that our framework produces solutions that are robust to poor initial conditions as well as difficult to reach contacts. The plug-and-play capability awarded by our transfer method makes it especially well suited for manipulator prototyping, which we illustrate in concluding experiments. Finally, we demonstrate a synthesized grasp solution on a physical, custom designed robot hand.

II. RELATED WORK

Numerous prior efforts have targeted the problem of recovering and optimizing manipulator pose from contacts, the majority of which can be broadly classified under either single point or area based approaches.

Single point methods use individual object points as the basis for extracting the corresponding hand configuration. Mapping individual object and hand contact points allows for the use of traditional inverse kinematics [34], [35]; however, in grasps that contain a large number of contacts, the problem is generally overconstrained and may instead be best solved using an optimization approach where the user can specify the importance of different tradeoffs (e.g., match contacts, match hand pose, etc.). Optimization approaches can additionally incorporate kinematic constraints and endeavor to

¹Computer Science Department, Carnegie Mellon University

²Robotics Institute, Carnegie Mellon University

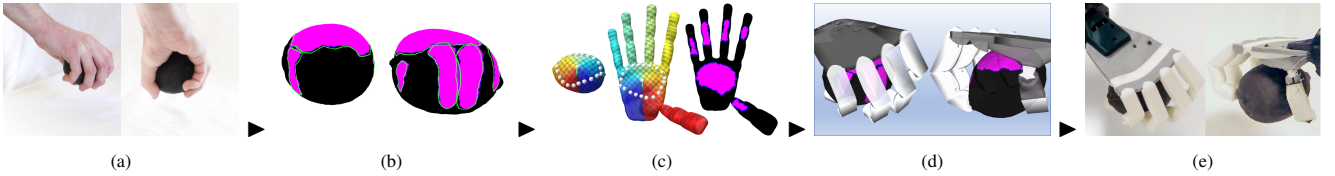


Fig. 1: High level overview of our framework. (a) Human demonstrations of grasps and manipulations are collected and (b) reconstructed using existing techniques. (c) Contact regions are then transferred from object to target manipulator, and (d) the whole hand kinematic pose is computed from the transferred contacts via optimization. (e) The robot hand then utilizes the final articulated solution.

find least-squares [35] or force-closure inducing [39], [44] solutions. But while these approaches are fast and straightforward, single point contacts are an idealized representation of real-world situations. Additionally, approximating contact areas as single points sacrifices useful information.

Consequently, some recent research efforts have turned instead to utilizing contact regions. Though a number of existing works have considered contacts purely through geometric reasoning, including independent contact regions [37], [28] and directly mapping individual links to mesh slices [38], recent data driven works have produced high fidelity contact maps by instead capturing contacts directly from human demonstrations [14] or synthesizing them from vision based retargeting and simulation [26]. These maps have subsequently been utilized to synthesize grasps for morphologically diverse manipulators [15] as well as optimize coarse estimates [21], [26]; however, owing to the difficulty of mapping contact regions to articulated manipulators, these methods are dependent on priors or exhaustive grasp sampling, which thus limit their robustness and speed.

This paper directly addresses the mapping problem by proposing a method to transfer object contact areas to any manipulator in a manner that fully preserves relative contact point distances regardless of underlying geometry, essentially merging the benefits of single point and area based techniques. We then show that the resulting contact area correspondence enables the use of a simple, yet robust optimization to compute the best matching, kinematically feasible hand pose. Our technique does not require sampling or priors and can be used on any hand design, and additionally is intentionally designed to allow full user control over both the transfer and optimization process, which we show leads to fast, robust, and qualitatively reasonable results for both static grasps and in-hand manipulations. We demonstrate results for a range of simulated robot hands, a graphical human hand, and a real robot hand custom designed for such tasks.

III. PROCEDURE

Our algorithm consists of several stages, roughly illustrated in Figure 1. First, thermal traces of contact patches generated from human grasps and manipulations are captured and reconstructed onto object meshes using techniques from prior works [14], [29]. The process outlined in this paper then transfers contact patches from object surfaces onto a “skin” of the manipulator, and subsequently projects contacts from the skin onto the articulated hand. Finally, we utilize

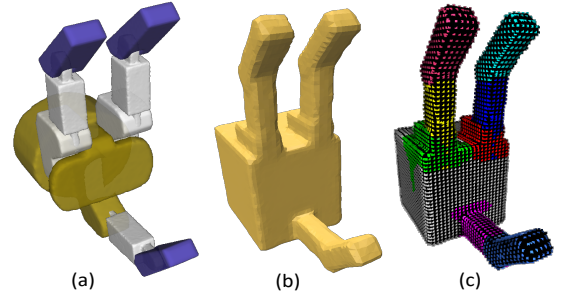


Fig. 2: The (a) articulated Barrett Hand can be (b) approximately skinned by stitching together primitive collision geometries. (c) The projection process partitions the skin into groups based on the link locations of the articulated hand.

the mapping to compute grasps and manipulations with the target manipulator that best match the correspondence. Each stage is described in detail in the proceeding subsections.

A. Contact Capture, Reconstruction, and Tracing

Contact regions resulting from human grasps are first captured using a combination of thermochromic spray painted objects and RGBD imaging, and subsequently mapped onto object mesh surfaces using a reconstruction process detailed in existing works [14], [29]. Regions are then annotated and processed into *patches*, which are represented by a single *root* (*PR*) mesh vertex and collection of *boundary* (*PB*) mesh vertices. Boundaries are then down-sampled to produce *interpolation boundary* (*IB*) sets of 20-30 mesh vertices, which are then traced from initial to final positions in the case of manipulations. Detailed definitions and process descriptions are available in [29].

B. Skinning and Projection

Geometry processing algorithms are typically designed to operate over connected surfaces; however, the large majority of robotic systems are articulated, comprised instead of independent surface links connected by joints. These surfaces may also exhibit degenerate characteristics, including non-manifold edges, obtuse triangles, and near-zero area faces, which, combined with articulation, render many geometry processing algorithms useless.

Therefore, we instead construct a fully manifold “skin” of each manipulator and then project vertices from the skin back on to the original articulated geometry using KD tree [13] approximation. Figure 2 illustrates the skinning and projection process. In particular, we note that skins can be constructed from even coarse mesh approximations such as

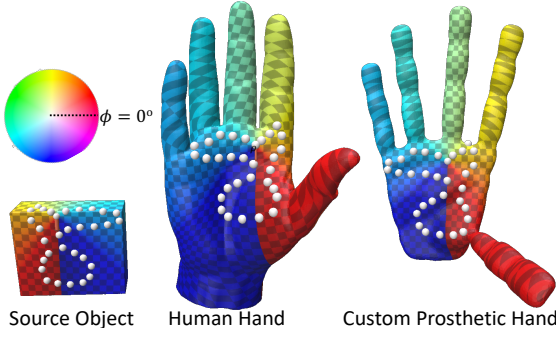


Fig. 3: Illustration of our logmap-based contact patch transfer process. Accurate relative distances and angles at all mesh vertices enable transfer of even large, irregularly shaped patches to widely differing hand geometries.

primitive collision geometries. Post projection, points on the skin which have no nearby articulated vertex below threshold ϵ are ignored during optimization. We use Blender [18] with the Phobos attachment to construct skins and the Open3d library [45] to perform the projection.

C. Contact Patch Transfer

The key idea of our transfer process is that patch shapes on the object and manipulator are roughly equivalent, regardless of the surface on to which they are projected. More formally, the distance and direction of the IB points from the root should be preserved under a geometry independent logarithmic map $\mathbf{L}_{r,\phi}$ [42]. We therefore require four parameters, all of which are visually adjustable by the user: the patch's root vertex on the hand skin $\mathbf{v}_{r,h}$ and object $\mathbf{v}_{r,o}$, as well as the tangent vector direction from the hand $\vec{\mathbf{v}}_{r,h}$ and object $\vec{\mathbf{v}}_{r,o}$ in which to begin the sweep. The corresponding IB set on the hand can then be entirely computed as:

$$\begin{aligned} \mathbf{v}_{IB_i,h}^* = \arg \min_{\mathbf{v}_h} & \quad \|\mathbf{L}_{r,\phi}(\mathbf{v}_h) - \mathbf{L}_{r,\phi}(\mathbf{v}_o)\|_2^2 \\ \text{s.t.} & \quad \mathbf{L}_{r,\phi}(\mathbf{v}_h) = f(\mathbf{v}_{r,h}; \vec{\mathbf{v}}_{r,h}) \\ & \quad \mathbf{L}_{r,\phi}(\mathbf{v}_o) = f(\mathbf{v}_{r,o}; \vec{\mathbf{v}}_{r,o}) \end{aligned} \quad (1)$$

Finding these correspondences thus requires computation of logmap coordinates (r, ϕ) for all vertices on both object and skin. Naively, these quantities can be computed by tracing geodesics from the root to all vertices (r) and propagating the root tangent vector via parallel transport (ϕ) [22]; unfortunately, these operations are notoriously expensive. The Vector Heat Method proposed by Sharp et. al. [42], however, reduces to seconds the parallel transport of *both* divergence and root tangent vectors through the use of short time heat diffusion. As Figure 3 illustrates, this method can successfully transfer patches of arbitrary shape on to widely differing surface geometries, can be performed in seconds, and guarantees both relative distance and angle preservation. We use the Polyscope viewer [41] and Geometry Central library [40] to enable user selection of $(\mathbf{v}_{r,h}; \mathbf{v}_{r,o}; \vec{\mathbf{v}}_{r,h}; \vec{\mathbf{v}}_{r,o})$, solve Eq. 1, and export the final mapping.

D. Extension to Manipulations

We note that the aforementioned procedure can only transfer static grasps; however, manipulations require dynamic

contacts capable of moving, appearing, or disappearing from the hand at any time. To account for this behavior, we first transfer initial and final grasps and then adopt the procedure of Lakshmipathy et. al. [29] to evolve patches on the hand in conjunction with evolution of patches on the object.

E. Optimization Procedure

Computing the associated IB mappings between the object and hand enabled use of a straightforward, three-term optimization problem to determine the best kinematic hand pose θ^* :

$$\begin{aligned} \theta^* = \arg \min_{\theta} & \quad \sum_{i=0}^N \Gamma_{D,i} + \lambda_n \Gamma_{N,i} + \lambda_p \Gamma_{P,i} \\ \text{s.t.} & \quad \theta_L \leq \theta \leq \theta_U \end{aligned} \quad (2)$$

where θ is the degree of freedom vector, θ_L and θ_U are the lower and upper bounds of each degree of freedom respectively, $\Gamma_{D,i}$, $\Gamma_{N,i}$, and $\Gamma_{P,i}$ are the distance, normal, and prior pose deviation penalty terms for each corresponding pair of points i respectively, and λ_n and λ_p are weighting hyperparameters. Each penalty term is elaborated upon in the proceeding paragraphs.

First, we introduce $\Gamma_{D,i}$ to minimize the L_2 distance between each pair i of corresponding hand and object contacts:

$$\Gamma_{D,i} = \|\mathbf{p}_{o,i} - \mathbf{p}_{h,i}(\theta)\|_2^2 \quad (3)$$

and $\Gamma_{N,i}$ to encourage anti-alignment of vertex normals:

$$\Gamma_{N,i} = (1 + \mathbf{n}_{h,i}(\theta) \cdot \mathbf{n}_{o,i})^2 \quad (4)$$

where each pair of object and hand contact points are denoted by o, i and h, i respectively, and hand point locations as well as vertex normal orientations are determined by the current hand pose θ .

We additionally introduce a third term to penalize deviation from θ_P , a hand pose prior for the current simulation:

$$\Gamma_{P,i} = \|\theta - \theta_P\|_2^2 \quad (5)$$

θ_P jointly serves two purposes. At the start of the optimization, θ_P is set to the default pose, thereby penalizing rest pose deviation during the first set of iterations. During subsequent calls, θ_P is by default set to the optimal solution from the last set of iterations; however, if the user edits the default guess (e.g. moves a finger, drags the palm, etc.), θ_P is instead set to the user edited pose. As a result, $\Gamma_{P,i}$ evolves as the optimization proceeds to reflect current progress and user direction.

It is worth noting that Eq. 2 does not contain a collision penalty term as suggested by several prior works [15], [32], [23]. Omission of this term is intentional and ultimately led to both substantial drops in solution discovery time as well as improvements in the proposal of solutions for difficult contact maps (see Figure 8).

The fully differentiable nature and cheap computation cost of Eq. 2 allows utilization of fast, gradient based solvers even using numerical gradient approximation; however, we

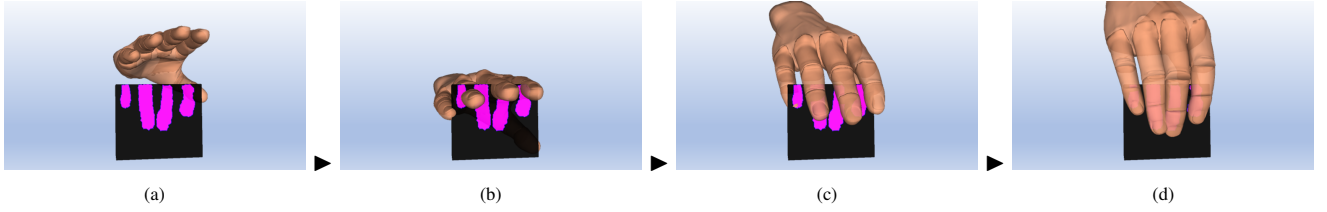


Fig. 4: Optimization progress for finding a feasible box power grasp at (a) 0, (b) 250, (c) 800, and (d) 1,000 iterations.

empirically found that different solvers provided slightly different solutions depending on both θ_P and the object transform. We ultimately settled on the Method of Moving Asymptotes [43] for generating the majority of our results, though other solvers were occasionally used as well. Each method was capped at 1,000 iterations per optimization call to intermittently update θ_P and allow the user to edit intermediate estimates using IK. Figure 4 illustrates successive guesses over the course of a single optimization call. We used the NLOpt library [27] for defining and solving Eq. 2.

IV. RESULTS

Similar to Brahmbhatt et. al. [15], we performed a series of experiments using four different manipulators - a 20 degree of freedom human hand [33], an Allegro hand [9], a Barrett hand [1], and a custom made anthropomorphic prosthetic hand - across several static grasps and manipulations of common household items. Items and contact maps were borrowed from several existing datasets, including ContactDB [14], Contact Tracing [29], and YCB [17]. The primary desiderata were speed and scalability, robustness, and flexibility to accommodate design or intermediate optimization modifications. Only results for qualitatively reasonable grasps are reported. All simulations were conducted using the Dynamic Animation and Robotics Toolkit (DART) [30].

A. Grasps and Manipulations

Figure 5 provides a collage of static grasps generated using our contact transfer procedure, while Figure 6 illustrates a manipulation sequence used to pull a box of sugar off a kitchen shelf. Note that in a number of cases the manipulator does not possess the required dexterity to successfully reach the contacts; however, the combination of our contact transfer and optimization procedure, along with ability to accommodate interactive user refinement during the process, results in kinematically feasible “best effort” solutions across a variety of manipulators and objects.

B. Computation Speed

To test the speed and scalability of our algorithm, we examined the time taken by each manipulator to reach a qualitatively reasonable solution across objects containing variable numbers of contact patches. Each trial of four hands was performed with respect to a single object averaged over three separate initial object placements. Objects were swapped between trials if the appropriate number of patches was not available. All hands were initialized to their default start positions. Parenthetical quantities indicate degrees of

freedom, and no more than 6 patches were used (1 per human finger + palm). Each hand includes 6 additional degrees of freedom due to a free root joint, while the Barrett hand’s ordinarily constrained degrees of freedom are relaxed for the purposes of simulation. All tests were run on a single Intel Xeon W-1250 3.3 Ghz processor without the use of GPU acceleration or parallel computation.

Grasp Synthesis Speed Comparison - Favorable Initialization				
	3 patches	4 patches	5 patches	6 patches
Human Hand (26)	0.688 s / 0 edits	0.884 s / 0.33 edits	0.422 s / 1 edit	1.036 s / 1 edit
Allegro Hand (22)	0.135 s / 0 edits	0.303 s / 0 edits	0.278 s / 1 edit	N/A
Barrett Hand (14)	0.072 s / 0 edits	0.088 s / 0 edits	N/A	N/A
Prosthetic (22)	0.288 s / 0 edits	0.346 s / 0.33 edits	0.284 s / 0.67 edits	0.394 s / 1 edit

TABLE I: Speed test comparison of 4 different manipulators of varying degrees of freedom with favorable initialization.

Grasp Synthesis Speed Comparison - Poor Initialization				
	3 patches	4 patches	5 patches	6 patches
Human Hand (26)	1.115 s / 0 edits	1.752 s / 0.67 edits	1.406 s / 1.33 edits	2.032 s / 2.33 edits
Allegro Hand (22)	0.397 s / 0 edits	0.721 s / 0.67 edits	0.522 s / 1 edit	N/A
Barrett Hand (14)	0.133 s / 0 edits	0.174 s / 0 edits	N/A	N/A
Prosthetic (22)	0.441 s / 0 edits	1.443 s / 0.67 edits	0.564 s / 1.33 edits	1.267 s / 1.67 edits

TABLE II: Speed test comparison of 4 different manipulators of varying degrees of freedom with poor initialization.

Tables I and II tabulate both the average total times taken across all optimization calls as well as the number of intermediate user edits made to θ_P during the process. Note that these reported values only consider a small sample size and that variance between different objects and regions of contact is high; however, they do reveal some interesting trends. As expected, greater computation time and interventions are generally required for higher degree of freedom manipulators; however, it is surprising that solution search time did not necessarily increase with more contacts. A possible explanation is that additional contacts may heavily favor certain classes of solutions, and by doing so enable faster local minima convergence; however, additional experiments over larger numbers of objects and contact distributions are required to thoroughly test the conjecture.

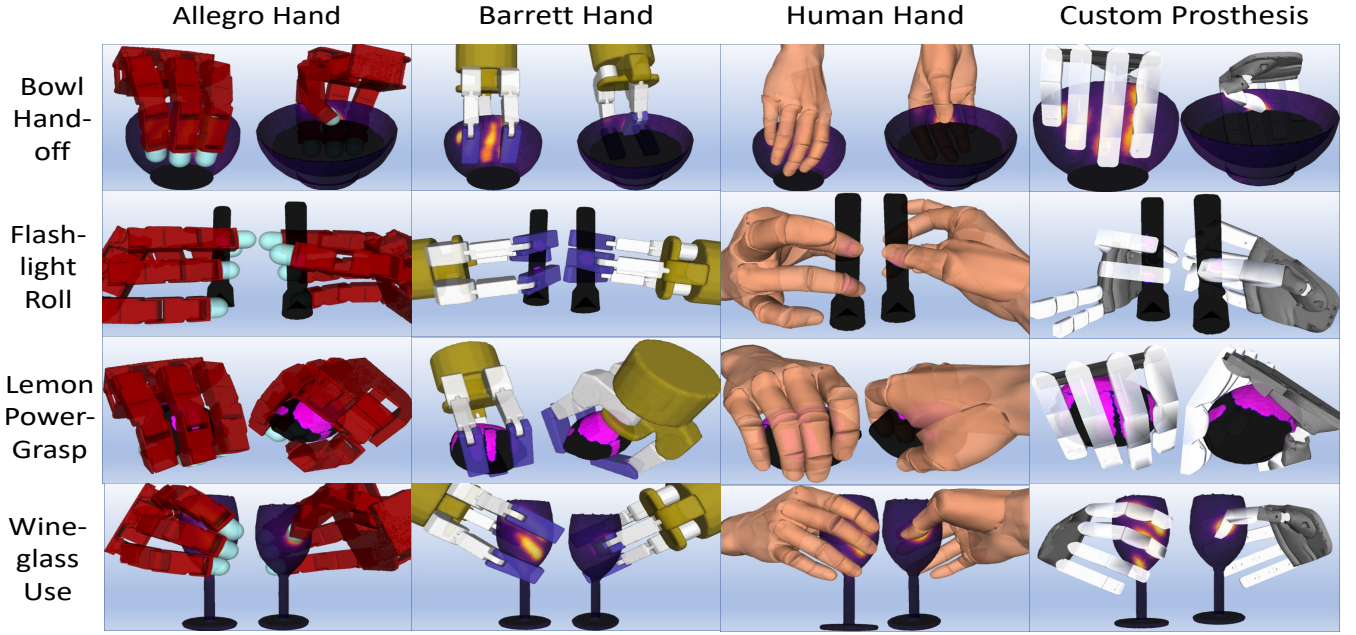


Fig. 5: Grasps synthesized as a result of our transfer procedure across a variety of kinematically diverse manipulators, objects, and grasps.

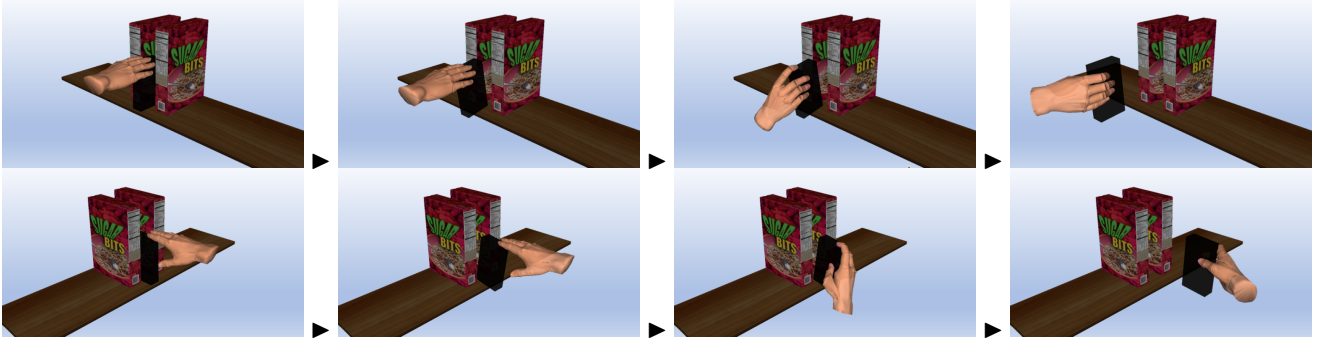


Fig. 6: Demonstration of using the method to quickly approximate a kinematic grasp time series spanning a full simple manipulation of pulling a box of sugar off a kitchen shelf. Poses for successive manipulation steps can be generated at real-time speeds due to the inclusion θ_p and contact evolution time series data.

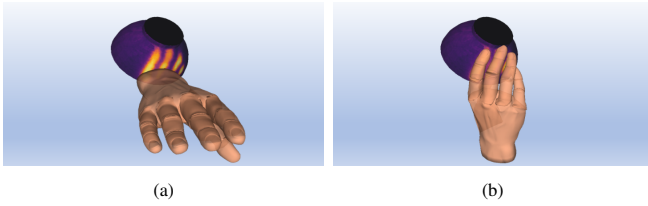


Fig. 7: Results of our method in a configuration where the target object is inverted and placed behind the manipulator. Despite poor initialization (a), our method still finds an acceptable solution after only a few optimization calls (b).

C. Robustness to Poor Initialization

Figure 7 shows the start state and ending grasp of the human hand after running our optimization framework for exactly two optimization calls comprised of 1,000 maximum iterations each, with each round converging and terminating in seconds with no edits. We repeated the procedure for several other poor object and hand initial states and found

the behavior to be relatively consistent regardless of the manipulator and object used. As a result, our method is well suited to support dynamic object placement in a plug-and-play manner.

D. Robustness to Difficult Grasps

Figure 8 illustrates the outcome of synthesizing a kinematically feasible grasp in between the holes of a pair of scissors. All solutions were found starting from default rest poses, and no edits were made to θ_P between calls. While the human hand and custom prosthetic produced reasonable solutions, the Allegro and Barrett Hand noticeably appear too large to find a feasible solution.

Despite the grasp’s irregularity and the fact that contacts are in hard to reach places, our framework still does a reasonable job in finding solutions quickly and reliably. In the case of the Barrett and Allegro Hand, the framework also provides useful information through fast failure, which can immediately prompt design changes during early stages of prototyping. Finally, due to the irregularity of the grasp and

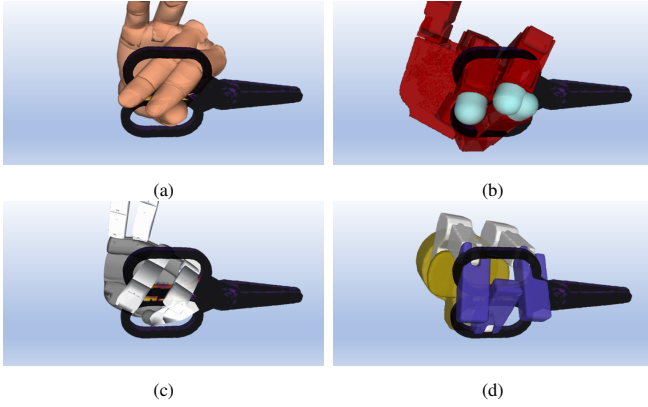


Fig. 8: Results of our method in finding solutions for a difficult grasp in between the holes of a pair of scissors. The (a) human hand and (c) custom prosthetic found plausible solutions, while the (b) allegro hand and (d) barrett hand failed due to the dimensions being too large for the object.

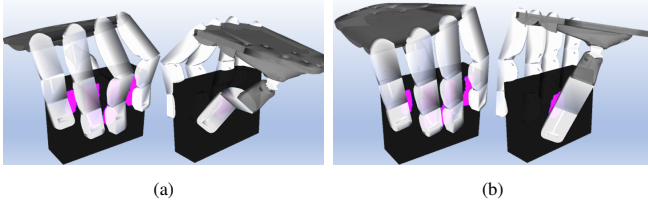


Fig. 9: Custom human hand prosthesis demonstration during a box manipulation in which (a) the index finger, middle finger, and thumb joints are allowed to overextend with negative joint limits and (b) when stricter limits are imposed. Note that this alteration changes the whole hand solution rather than only the impacted joints.

hard to reach contact locations, we note that grasp sampling methods would typically fail to find a solution, in contrast to our method which still manages to do so.

E. Fast Reaction to Alterations

Figure 9 illustrates the results of running the same optimization procedure with our custom prosthesis, in which the joint limits are changed on-the-fly. In particular, we note the impact of joint limit adjustments not only on the impacted kinematic chains, but on the entire hand pose. We especially highlight the value of the latter observation within prototyping contexts since it amplifies the impact of even small design changes, which would otherwise be difficult and time-consuming to identify through existing methods.

F. Robot Demonstration

To demonstrate the utility of our approach with respect to prototyping real robot hand designs, we built a custom prosthesis using only a 3d FDM-printer, Thermoplastic Polyurethane (TPU) filament and brushless DC motors. We use a Flashforge Creator Pro 2 [3] retrofit with Flexion Extruders [2] to print the hand in one single part from soft and flexible filaments of varying shore hardness (Ninjatek Cheetah = 95A and Ninjatek Chinchilla = 75A) [4], [5]. The fingers are actuated by tendons (monofilament nylon fishing line) that are routed through channels printed inside the hand. Joint-like kinematics are achieved either by a combination of more rigid and soft materials or by creating

local geometric features such as bumps or creases on the hand. For instance, a good approximation of revolute joints is given by a crease coinciding with the joint-axis that runs across the finger or the palm. To accommodate more complex joints with more than one DoF we create rigid-soft-rigid layered features where the softer material acts as cartilage to allow for deformation along multiple axes. We place these features along the kinematic chain and investigate the potential of the hand to successfully grasp or manipulate objects. Discrepancies between simulated and real prosthesis resulting from under-actuation and soft material deformation can be reduced by selecting reasonable joint limits as shown in Figure 9. We show that we can successfully transfer a grasp generated by our method to the real hand in Figure 1 (e). Further grasps are provided in the supplemental video.

V. CONCLUSIONS AND FUTURE WORK

In summary, we have presented a direct, multi-contact transfer framework that can accommodate arbitrary contact regions, objects, and manipulators. We have also presented an optimization procedure that utilizes the transferred results to produce both static grasps and manipulations quickly, reliably, and reactively to user interaction. Our method provides kinematically feasible solutions without the use of grasp sampling or trained models, and by incorporating user feedback also enables discovery of better solutions without getting stuck in local minima. We have intentionally designed our approach to augment user capabilities, enabling full control over both the transfer and optimization process with responsive adaptation. Finally, we have shown that our method is especially useful for early stage manipulator prototyping, providing the first ground truth data driven means of testing the impact of design parameters on the kinematics of whole hand grasps in a plug-and-play manner, while at the same time being robust to difficult to reach contacts and dynamic object placement.

However, because this paper only considers kinematic approximation of rigid hands, our next research thrusts would be to extend the framework to consider physical characteristics of the grasp (e.g., ability to apply or resist task specific forces, force-closure, etc.), as well as adapt the procedure to soft hands. The former would enable us to evolve our kinematically feasible solutions to dynamically feasible solutions, while the latter will aid in the creation of the first multi-contact, ground truth data driven soft hand kinematic and dynamic approximation framework, which would be of aid to the soft robotics community. We are confident that the foundations laid by this paper will assist in both endeavors, and are excited to showcase the results of both thrusts in the future.

ACKNOWLEDGMENTS

This research was partially supported by the National Science Foundation award CMMI-1925130 and by a fellowship from Carnegie Mellon University’s Center for Machine Learning and Health awarded to Dominik Bauer.

REFERENCES

- [1] B. tech. barrett hand. <https://advanced.barrett.com/barrethand>. Accessed: 2021-09-08.
- [2] Diabase engineering - flexion extruder. <https://www.diabasemachines.com/flexion-shop>. Accessed: 2021-09-08.
- [3] Flashforge creator pro 2 - fdm printer with independent dual extruder (idex) system. <https://www.flashforge.com/product-detail/51>. Accessed: 2021-09-08.
- [4] Ninjatek cheetah. <https://ninjatek.com/shop/cheetah/>. Accessed: 2021-09-08.
- [5] Ninjatek chinchilla. <https://ninjatek.com/shop/chinchilla/>. Accessed: 2021-09-08.
- [6] Prencilia s.r.l. <https://www.prencilia.com/portfolio/mia/>. Accessed: 2021-09-08.
- [7] Shadow robot company: Dexterous hand series. <https://www.shadowrobot.com/dexterous-hand-series/>. Accessed: 2021-09-08.
- [8] Technical university darmstadt: Gripper gl. <http://www.thelaraproject.com/G1.html>. Accessed: 2021-09-08.
- [9] Wonik robotics: Allegro hand. <https://www.wonikrobotics.com/research-robot-hand>. Accessed: 2021-09-08.
- [10] OpenAI: M. Andrychowicz, B. Baker, M. Chociej, R. Jozefowicz, B. McGrew, J. Pachocki, A. Petron, M. Plappert, G. Powell, A. Ray, et al. Learning dexterous in-hand manipulation. *The International Journal of Robotics Research*, 39(1):3–20, 2020.
- [11] D. Antotsiou, G. Garcia-Hernando, and Kim T. K. Task-oriented hand motion retargeting for dexterous manipulation imitation. *arXiv preprint arXiv:1810.01845*, 2018.
- [12] D. Bauer, C. Bauer, J. P. King, D. Moro, K.-H. Chang, S. Coros, and N. Pollard. Design and control of foam hands for dexterous manipulation. *International Journal of Humanoid Robotics*, 17(01):1950033, 2020.
- [13] J. L. Bentley. Multidimensional binary search trees used for associative searching. *Communications of the ACM*, 18(9):509–517, September 1975.
- [14] S. Brahmabhatt, C. Ham, C. C. Kemp, and J. Hays. ContactDB: Analyzing and predicting grasp contact via thermal imaging. In *The IEEE Conference on Computer Vision and Pattern Recognition (CVPR)*, 6 2019.
- [15] S. Brahmabhatt, A. Handa, J. Hays, and D. Fox. ContactGrasp: Functional Multi-finger Grasp Synthesis from Contact. In *2019 IEEE/RSJ International Conference on Intelligent Robots and Systems (IROS)*, 2019.
- [16] S. Brahmabhatt, C. Tang, C. D. Twigg, C. C. Kemp, and J. Hays. ContactPose: A dataset of grasps with object contact and hand pose. In *The European Conference on Computer Vision (ECCV)*, August 2020.
- [17] B. Calli, A. Singh, A. Walsman, S. Srinivasa, P. Abbeel, and A. M. Dollar. The ycb object and model set: Towards common benchmarks for manipulation research. In *2015 International Conference on Advanced Robotics (ICAR)*, pages 510–517, 2015.
- [18] Blender Online Community. *Blender - a 3D modelling and rendering package*. Blender Foundation, Stichting Blender Foundation, Amsterdam, 2018.
- [19] M. Diftler, K. C. Jenks, and L. E. P. Williams. Robonaut: a telepresence-based astronaut assistant. In Matthew R. Stein, editor, *Telem manipulator and Telepresence Technologies VIII*, volume 4570, pages 142–152. International Society for Optics and Photonics, SPIE, 2002.
- [20] G. Garcia-Hernando, E. Johns, , and T. K. Kim. Physics-based dexterous manipulations with estimated hand poses and residual reinforcement learning. In *2020 IEEE/RSJ International Conference on Intelligent Robots and Systems (IROS)*, 2020.
- [21] P. Grady, C. Tang, C. D. Twigg, M. Vo, S. Brahmabhatt, and C. C. Kemp. ContactOpt: Optimizing contact to improve grasps. In *The IEEE Conference on Computer Vision and Pattern Recognition (CVPR)*, 2021.
- [22] H.W. Guggenheimer. *Differential Geometry*. Dover Books on Mathematics. Dover Publications, 2012.
- [23] C. Hazard, N.S. Pollard, and S. Coros. Automated design of manipulators for in-hand tasks. In *2018 IEEE-RAS 18th International Conference on Humanoid Robots (Humanoids)*, pages 1–8, 2018.
- [24] U. Hillenbrand and M. A. Roa. Transferring functional grasps through contact warping and local replanning. In *2012 IEEE/RSJ International Conference on Intelligent Robots and Systems*, pages 2963–2970, 2012.
- [25] Z. Jia, M. Lin, Z. Chen, and S. Jian. Vision-based robot manipulation learning via human demonstrations. *arXiv preprint arXiv:2003.00385*, 2020.
- [26] H. Jiang, S. Liu, J. Wang, and X. Wang. Hand-object contact consistency reasoning for human grasps generation. *arXiv preprint arXiv:2104.03304*, 2021.
- [27] S.G. Johnson. The NLOpt nonlinear-optimization package, 2017.
- [28] R. Krug, D. Dimitrov, K. Charusta, and B. Iliev. On the efficient computation of independent contact regions for force closure grasps. In *2010 IEEE/RSJ International Conference on Intelligent Robots and Systems*, pages 586–591, 2010.
- [29] A. Lakshmipathy, D. Bauer, and N. S. Pollard. Contact Tracing: A Low Cost Reconstruction Framework for Surface Contact Interpolation. In *2021 IEEE/RSJ International Conference on Intelligent Robots and Systems (IROS)*, 2021.
- [30] J. Lee, M. X. Grey, S. Ha, T. Kunz, S. Jain, T. Ye, S. S. Srinivasa, M. Stilman, and C. K. Liu. Dart: Dynamic animation and robotics toolkit. *Journal of Open Source Software*, 3(22):500, 2018.
- [31] Y. Li, J. L. Fu, and N. S. Pollard. Data-driven grasp synthesis using shape matching and task-based pruning. *IEEE Transactions on Visualization and Computer Graphics*, 13(4):732–747, 2007.
- [32] A. Meixner, C. Hazard, and N.S. Pollard. Automated design of simple and robust manipulators for dexterous in-hand manipulation tasks using evolutionary strategies. In *2019 IEEE-RAS 19th International Conference on Humanoid Robots (Humanoids)*, pages 281–288, 2019.
- [33] A.T. Miller and P.K. Allen. Graspit! a versatile simulator for robotic grasping. *IEEE Robotics Automation Magazine*, 11(4):110–122, 2004.
- [34] N.S. Pollard. Parallel algorithms for synthesis of whole-hand grasps. In *Proceedings of International Conference on Robotics and Automation*, volume 1, pages 373–378 vol.1, 1997.
- [35] S. Qiu and M. R. Kermani. Inverse kinematics of high dimensional robotic arm-hand systems for precision grasping. *Journal of Intelligent & Robotic Systems*, 101, 04 2021.
- [36] A. Rajeswaran, V. Kumar, A. Gupta, G. Vezzani, J. Schulman, E. Todorov, and S. Levine. Learning Complex Dexterous Manipulation with Deep Reinforcement Learning and Demonstrations. In *Proceedings of Robotics: Science and Systems (RSS)*, 2018.
- [37] M. A. Roa and R. Suarez. Computation of independent contact regions for grasping 3-d objects. *IEEE Transactions on Robotics*, 25(4):839–850, 2009.
- [38] C. Rosales, L. Ros, J. M. Porta, and R. Suárez. Synthesizing grasp configurations with specified contact regions. *The International Journal of Robotics Research*, 30(4):431–443, 2011.
- [39] C. Rosales, R. Suárez, M. Gabiccini, and A. Bicchi. On the synthesis of feasible and prehensile robotic grasps. In *2012 IEEE International Conference on Robotics and Automation*, pages 550–556, 2012.
- [40] N. Sharp, K. Crane, et al. geometry-central, 2019. www.geometry-central.net.
- [41] N. Sharp et al. Polyscope, 2019. www.polyscope.run.
- [42] N. Sharp, Y. Soliman, and K. Crane. The vector heat method. *ACM Trans. Graph.*, 38(3), 2019.
- [43] K. Svanberg. A class of globally convergent optimization methods based on conservative convex separable approximations. *SIAM Journal on Optimization*, pages 555–573.
- [44] Y. Ye and C. K. Liu. Synthesis of detailed hand manipulations using contact sampling. *ACM Trans. Graph.*, 31(4):1–10, 2012.
- [45] Q. Zhou, J. Park, and V. Koltun. Open3D: A modern library for 3D data processing. *arXiv:1801.09847*, 2018.
- [46] H. Zhu, A. Gupta, A. Rajeswaran, S. Levine, and V. Kumar. Dexterous manipulation with deep reinforcement learning: Efficient, general, and low-cost. pages 3651–3657, 05 2019.